

Effect of Ellipticity on Thermal Transport in ECH Plasmas in LHD

Hiroshi YAMADA, Masayuki YOKOYAMA, Sadayoshi MURAKAMI¹⁾, Kiyomasa WATANABE, Hisamichi FUNABA, Yoshiro NARUSHIMA, Satoru SAKAKIBARA, Tomohiro MORISAKI, Yoshio NAGAYAMA, Shin KUBO, Takashi SHIMOZUMA, Kenji TANAKA, Tokihiko TOKUZAWA, Ichihiro YAMADA and LHD Experimental Group

National Institute for Fusion Science, 322-6 Oroshi-cho, Toki 509-5292, Japan

¹⁾*Department of Nuclear Engineering, Kyoto University, Yoshida-honmachi, Sakyo, Kyoto 606-8501, Japan*

(Received 9 December 2007 / Accepted 12 February 2008)

Effect of ellipticity on thermal transport was investigated in ECH plasmas in LHD. Ellipticity κ is scanned from 0.8 to 1.4 by controlling the quadrupole magnetic field. Experimental data of energy confinement time align with the scaling for all configurations; however, there exist systematic offsets. Performance $\tau_E^{\text{exp}}/\tau_E^{\text{ISS04}}$ is summarized as 0.94 ± 0.02 for $\kappa = 0.8$, 1.41 ± 0.07 for $\kappa = 1.0$, and 0.91 ± 0.03 for $\kappa = 1.4$. Local transport analysis based on power balance indicates that the anomalous transport predominates the plasma transport. However, the observed anomaly shows correlation with the change in the effective helical ripple ε_{eff} . Physical background of this correlation and the dependence on the poloidal viscous damping rate C_p is discussed. The present experimental comparison suggests a negative evidence for the relevance of C_p .

© 2008 The Japan Society of Plasma Science and Nuclear Fusion Research

Keywords: thermal transport, configuration effect, neoclassical transport, anomalous transport, net-current free plasmas, ellipticity

DOI: 10.1585/pfr.3.S1032

1. Introduction

Exploration of the effect of magnetic configuration on confinement is a prerequisite for optimization of a helical system. Extensive experimental as well as theoretical investigations have been performed. Geometrical optimization for the neoclassical transport was demonstrated in NBI heated plasmas in LHD, and the anomalous transport was suppressed in the neoclassical optimized configuration [1]. In these configuration studies, the position of the magnetic axis is the key control parameter [2].

International collaboration for the stellarator/heliotron confinement database has progressed [3–6], and a comprehensive comparative study has suggested that net-current free plasmas have robust and similar dependence on magnetic field, density, and heating power [3–5]. For example, the ISS04 scaling [5]:

$$\tau_E^{\text{ISS04}} = 0.134 a^{2.28} R^{0.64} P^{-0.61} \bar{n}_e^{0.54} B^{0.84} \iota_{2/3}^{0.41},$$

where a and R are the minor and major radii in m, P is the heating power in MW, \bar{n}_e is the line averaged density in 10^{19} m^{-3} , B is the magnetic field in T, and $\iota_{2/3}$ is the rotational transform at the two-thirds radius, can describe the trend of energy confinement time in a variety of devices quite well. This expression is rephrased into non-dimensional parameters in the following:

$$\tau_E^{\text{ISS04}}/\tau_{\text{Bohm}} = \rho^{*-0.79} \beta^{-0.19} \gamma_b^{*0.00} \iota_{2/3}^{1.06} \varepsilon^{-0.07},$$

author's e-mail: hyamada@LHD.nifs.ac.jp

where τ_{Bohm} is the Bohm diffusion time, which is proportional to the magnetic field over temperature, ρ^* is the normalized gyro radius, γ_b^* is the collisionality normalized by the bounce frequency of a toroidal banana orbit, and ε is an inverse aspect ratio (a/R). The dependence close to ρ^{*-1} indicates that the confinement is characterized by the gyro-Bohm nature governed by turbulence with a short wave-length scaled by the gyro radius. Together with confirmation of this commonality, existence of systematic offsets between different configurations/devices was pointed out. These device/configuration dependent offsets were quantified by comparisons of subsets reflecting characteristic configurations; however, physical background of this quantity has not been clarified yet. The measure of the offsets correlates with the effective helical ripple ε_{eff} , which is characterized by the neoclassical helical ripple transport in the collisionless $1/\nu$ regime [5]. It should be noted that the transport in experiments itself is significantly larger than the neoclassical transport. Since the anomalous transport is predominant, a physical picture of the neoclassical transport is not directly applicable to explain experimental observation. Therefore, these observations postulate a working hypothesis that the neoclassical optimization can suppress the anomalous transport.

Large flexibility of the coil system of LHD enables configuration scans other than the position of the magnetic axis, i.e., plasma elongation. Although the plasma elongation scans for NBI heated plasmas have already been reported [1], ECH plasmas located in the collisionless regime

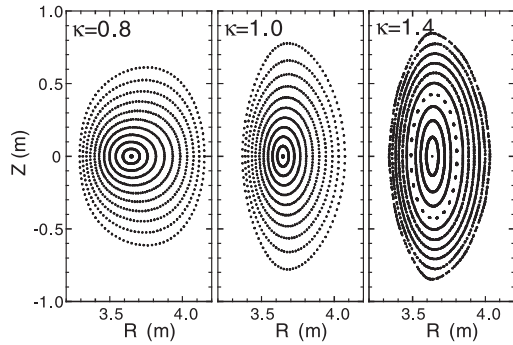


Fig. 1 Magnetic flux surfaces for an elongation scan. Cross-section at a vertically elongated position where the helical coils are located on the equatorial plane.

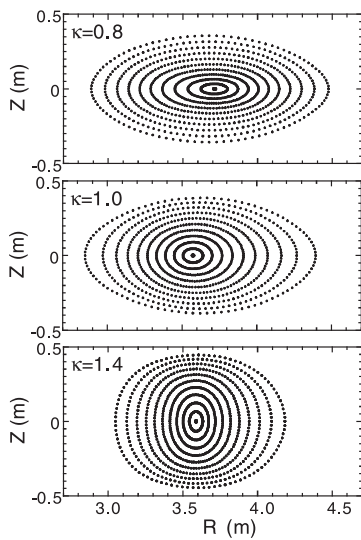


Fig. 2 Magnetic flux surfaces for an elongation scan. Cross-section at a horizontally elongated position where the helical coils are located on the top and bottom.

have not been studied yet.

2. Experimental Set-Up

Plasma elongation was controlled by the quadrupole field and scanned in the range between $\kappa = 0.8$ and 1.4 (see Figs. 1 and 2). Here, elongation is defined by the toroidal averaged value since the elliptic surface rotates along the toroidal angle. The position of the magnetic axis R_{ax} is fixed at 3.6 m.

The magnetic field is fixed at 1.5 T, which provides centrally well focused deposition of ECH with 84 GHz. All ECH power is deposited inside of $\rho = 0.2$, where ρ is the normalized minor radius. The plasma volume, i.e., the plasma minor radius is kept constant by controlling the effective aspect ratio of the helical coil. The helical coil consists of 3 blocks with independent power supplies, which can change the effective current center of the coil. Although the Shafranov shift and resultant change in rota-

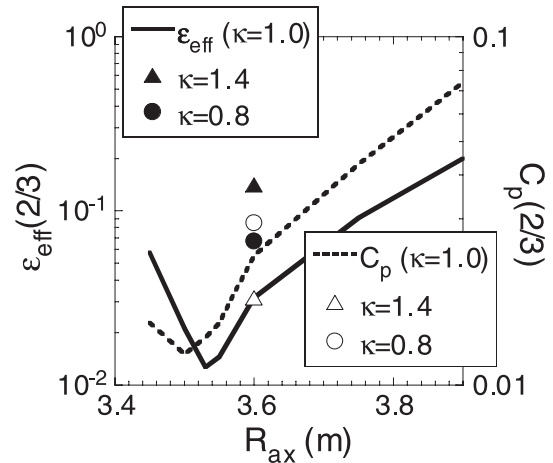


Fig. 3 Dependence of the effective helical ripple ε_{eff} and poloidal viscous damping rate C_p on the position of the magnetic axis. Elongation scans are plotted by triangles and circles at $R_{ax} = 3.6$ m.

tional transform is sensitive to ellipticity [7], finite- β effect is not significant in the present study since the β is limited to 0.3% in ECH plasmas.

In this study, the poloidal viscous damping rate is explored as a potential key parameter for connecting the neo-classical optimization and suppression of the anomalous transport. In general, zonal flows are generated efficiently in the configuration with low poloidal viscosity, and the suppression of the anomalous transport is anticipated in such a configuration. The poloidal viscous damping rate C_p [8] is plotted with ε_{eff} against R_{ax} in Fig. 3. Since C_p is affected by the toroidal curvature as ε_{eff} , C_p and ε_{eff} have a clear correlation. Indeed, in the standard ellipticity $\kappa = 1.0$, both quantities have the same trend against R_{ax} and become minimum in the vicinity of $R_{ax} \sim 3.6$ m, where high performance can be obtained in the experiment.

Therefore, which parameter, ε_{eff} or C_p , is more essential in transport cannot be determined. However, plasma elongation can separate these two effects. As seen in Fig. 3, a vertically elongated configuration ($\kappa = 1.4$) has larger ε_{eff} and smaller C_p than the standard configuration ($\kappa = 1.0$).

3. Experimental Results

Two-dimensionally similar discharges with different elongation were compared to clarify the elongation effect on heat transport. The line averaged density is controlled at $1 \times 10^{19} \text{ m}^{-3}$ (see Fig. 4). The electron temperature is also controlled to be the same in the two cases with $\kappa = 0.8$ and 1.0 by adjusting the heating power (see Fig. 5)

Here, it should be noted that the investigated plasmas lie in the $1/\nu$ regime, and they do not enter so deeply in collisionless regime that the electric field effect on the neo-classical transport is not significant. Since the case with $\kappa = 1$ shows the better confinement, the heating power is 0.93 MW for $\kappa = 0.8$ and 0.35 MW for $\kappa = 1$. The plasma

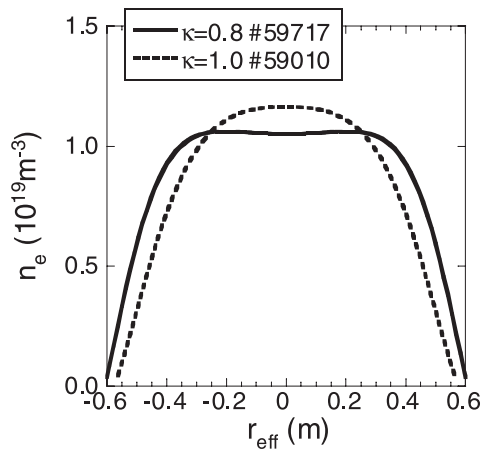


Fig. 4 Electron density profiles in discharges with different elongations.

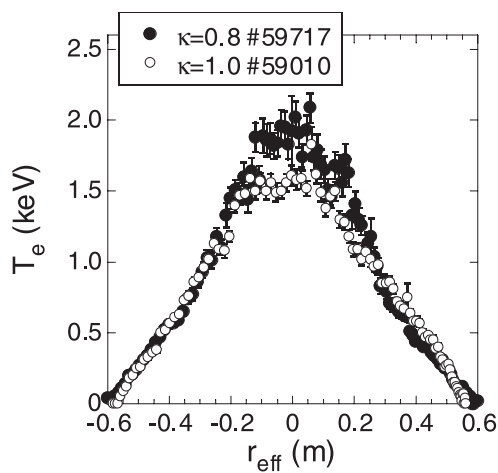


Fig. 5 Electron temperature profiles in discharges with different elongations.

parameters except for the elongation are similar to each other; therefore, representative non-dimensional physical parameters such as normalized gyro-radius ρ^* , collisionality ν^* , and beta are also similar to each other.

Figure 6 shows the ratio of the electron heat diffusivity in these two cases. Since the plasma parameters in these two cases are the same, the deviation of this ratio from 1 can be attributed to the remained difference, i.e., elongation. Corresponding to the global confinement nature, local heat diffusivity in the experiment, shown in a solid curve, indicates enhancement of heat transport in the case with $\kappa = 0.8$ by a factor of 2 to 3. A dotted line is the results from numerical calculation using GSRAKE [9] based on the neoclassical theory. The radial electric field is assumed to be zero in this calculation. Since ν_b^* , the collisionality of the plasmas studied here, ranges from 0.1 to 1, the effect of the radial electric field E_r is not significant. These two curves are close to each other, which suggest that the neoclassical transport may cause the difference in heat transport. However, this is not the case. Figure 7 shows the heat

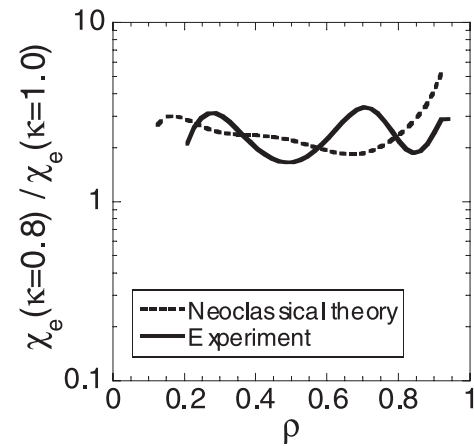


Fig. 6 Ratio of heat diffusivity of two discharges with different elongations.

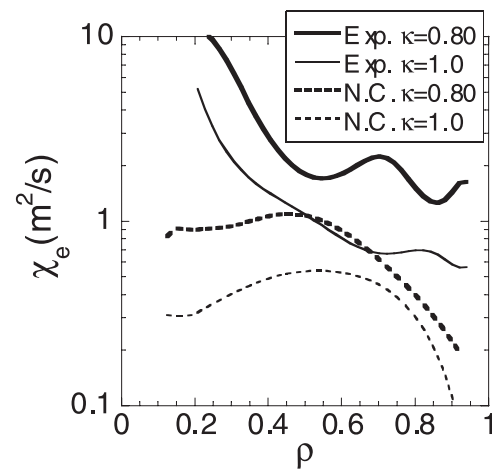


Fig. 7 Experimental and neoclassical heat diffusivity.

diffusivity profile. The fat solid curve is the experimental value in the case with $\kappa = 0.8$, and the dotted fat curve is the corresponding neoclassical prediction. The experimental value is significantly larger than the neoclassical value, which indicates that heat transport is anomalous even for the case with $\kappa = 0.8$. It should be noted that the neoclassical value indicated here exhibits the upper limit because of the assumption of $E_r = 0$. Therefore, this is another example that the configuration effect on the anomalous transport is correlated or accidentally coincides with the nature of neoclassical transport [5].

Figure 8 shows the comparison of experimental energy confinement time with the prediction from the ISS04 scaling for plasmas with different ellipticity as shown in Figs. 1 and 2. Energy confinement times have the maximum performance at $\kappa = 1$ and degrades in both prolate ($\kappa > 1$) and oblate ($\kappa < 1$) directions. These trends agree with the observation in NBI heated plasmas [2].

Experimental data align with the scaling for all configurations. Each performance $\tau_E^{\text{exp}}/\tau_E^{\text{ISS04}}$ is summarized as 0.94 ± 0.02 for $\kappa = 0.8$, 1.41 ± 0.07 for $\kappa = 1.0$, and

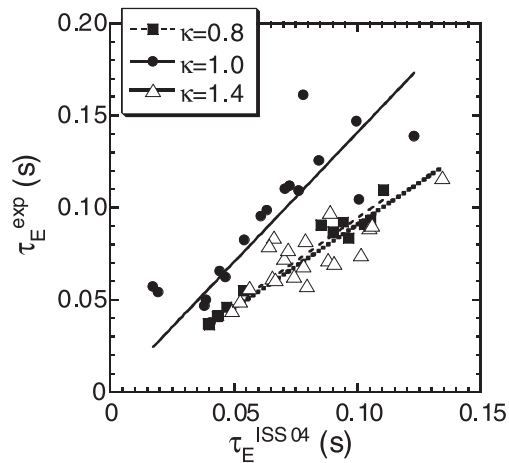


Fig. 8 Comparison of experimental energy confinement time with the prediction from the ISS04 scaling.

0.91 ± 0.03 for $\kappa = 1.4$. If C_p is the more relevant parameter, the confinement should be the maximum at $\kappa = 1.4$. However, the experiments indicate that the confinement is the best at $\kappa = 1.0$ and declined by both the prolate ($\kappa = 1.4$) and oblate ($\kappa = 0.8$) modifications. The present experimental comparison suggests a negative evidence for the relevance of C_p .

4. Conclusions

Effect of ellipticity on thermal transport was investigated for ECH plasmas in LHD. Ellipticity κ is scanned from 0.8 to 1.4 by controlling the quadrupole magnetic field. Experimental data of energy confinement time align with the scaling for all configurations; however, there exist systematic offsets. Performance $\tau_E^{\text{exp}}/\tau_E^{\text{ISS04}}$ is summarized as 0.94 ± 0.02 for $\kappa = 0.8$, 1.41 ± 0.07 for $\kappa = 1.0$, and 0.91 ± 0.03 for $\kappa = 1.4$. Local transport analysis based on power balance indicates that the anomalous transport predominates the plasma transport. However, the observed anomaly shows correlation with the change in the effective helical ripple ε_{eff} . Since ε_{eff} should not be directly linked

with the anomalous transport model, clarification of the configuration dependent parameters to bridge the anomalous transport and ε_{eff} is required for establishing the optimized magnetic configuration. In this study, the poloidal viscous damping rate is explored as a potential key parameter. In general, zonal flows are generated efficiently in the configuration with a low poloidal viscosity, and the suppression of the anomalous transport is anticipated in such a configuration. Since the poloidal viscous damping rate C_p is affected by curvatures that also reflect ε_{eff} , C_p and ε_{eff} generally have a correlation. Indeed, the inward shift of the magnetic axis causes suppression of both C_p and ε_{eff} simultaneously. However, plasma elongation can separate these two effects. Here elongation is defined by the toroidal averaged value. A vertically elongated configuration ($\kappa = 1.4$) has larger ε_{eff} and smaller C_p than the standard configuration ($\kappa = 1.0$). The experimental results indicate that the confinement is the best at $\kappa = 1.0$ and declined by both the prolate ($\kappa = 1.4$) and oblate ($\kappa = 0.8$) modifications. The present experimental comparison suggests a negative evidence for the relevance of C_p . In this study, ECH plasmas were investigated in detail. An earlier study on NBI heated plasmas also indicated that the energy confinement time has a similar dependence on ellipticity. Regardless of heating schemes, C_p is not supposed to be a relevant parameter to connect the neoclassical optimization and suppression of the anomalous transport.

- [1] H. Yamada *et al.*, Plasma Phys. Control. Fusion **43**, A55 (2001).
- [2] H. Yamada *et al.*, Nucl. Fusion **41**, 901 (2001).
- [3] U. Stroth *et al.*, Nucl. Fusion **36**, 1063 (1996).
- [4] H. Yamada *et al.*, Fusion Sci. Tech. **46**, 82 (2004).
- [5] H. Yamada *et al.*, Nucl. Fusion **45**, 1684 (2005).
- [6] A. Dinklage *et al.*, Nucl. Fusion **47**, 1265 (2007).
- [7] T. Kobuchi *et al.*, Plasma Phys. Control. Fusion **48**, 789 (2006).
- [8] C.D. Beidler *et al.*, Plasma Phys. Control. Fusion **36**, 317 (1994).
- [9] C.D. Beidler *et al.*, Plasma Phys. Control. Fusion **37**, 463 (1995).